Electrochemical Measurements with Interdigitated Array Microelectrodes

Yuzuru Iwasaki and
Masao Morita
NTT Basic Research Laboratories
Atsugi, Kanagawa
243-01, Japan

Interdigitated array (IDA) electrodes with different geometries were fabricated by a lithographic technique and used for determining reversible redox species. The high redox cycling collection efficiency of IDAs allowed sensitive electrochemical measurements with a high signal-to-noise ratio and a wide dynamic range. The detected current increased as the gap between the generator and the collector was reduced. Detection of 0.5 fmol (100 pM) of the neurotransmitter dopamine has been achieved using a 2-µm gap IDA electrode combined with liquid chromatography.

Electrochemical detection is coming into widespread use for the trace determination of easily oxidizable and reducible organic and inorganic compounds, because it provides a rather easy procedure for direct and selective detection. Recently, microelectrodes have been receiving attention in this field (1,2). They offer higher sensitivity than macroelectrodes of conventional size, because an electroactive molecule can approach the microelectrode from every direction (spherical diffusion). Therefore, the flux of electroactive molecules toward the electrode is much greater for a microelectrode than for a macroelectrode, for which the diffusion is planar.

Spherical diffusion has been utilized in sensor devices (3), detection of intermediate species, reaction analysis (4), electrochemistry in highly resistive media (5), and organic electronic devices (6). The characteristics of microelectrodes depend on their shapes and arrangements. Mathematical solutions for each kind of electrode response predict the superior electrode sensitivity of microelectrodes (7).

Although microelectrodes offer many advantages, they are not easy to construct, which limits their availability. They have been fabricated with metal or carbon wire in a glass tube by grinding the cross section of the tube, but this method has poor reproducibility and makes it difficult to control the electrode's shape. By using photolithography for the fabrication of microelectrodes, complex and arbitrary shapes and sizes of electrodes can be made with excellent reproducibility. This technique is also suitable for mass production of microelectrodes.

One of the most prominent examples of this kind of electrode is an interdigitated array (IDA) microelectrode. The IDA electrode consists of a pair of microband array electrodes that mesh with each other. Each set of microband electrodes in the IDA can be potentiostated individually, so a reduced species generated at one microband electrode diffuses across a small gap to the adjacent electrode, and then is oxidized and diffuses back to the original electrode. This redox cycling increases the currents at both electrodes. The concept of this electrochemical technique is similar to that at a rotating ring-disk electrode, but offers several advantages: steady-state currents can be achieved in a very short time, collection efficiency approaches unity, and handling and installing the electrode are simple. Pioneering work was done on the IDA by Sanderson and Anderson (8), and several applications have been reported (9–12). Tabei and co-workers have extensively studied the characteristics of the IDA electrode and its applications in electrochemistry (13). In this article, fundamental considerations and the applications of IDA electrodes in electrochemistry are described.

F1

Fabrication process of a metal IDA electrode.

(1) Photoresist coating on SiO_2 substrate.

(2) Lithographic patterning of photoresist.

(3) Metal film sputtering.

(4) Metal film patterning by lift-off method.

(5) Windowing by photoresist.

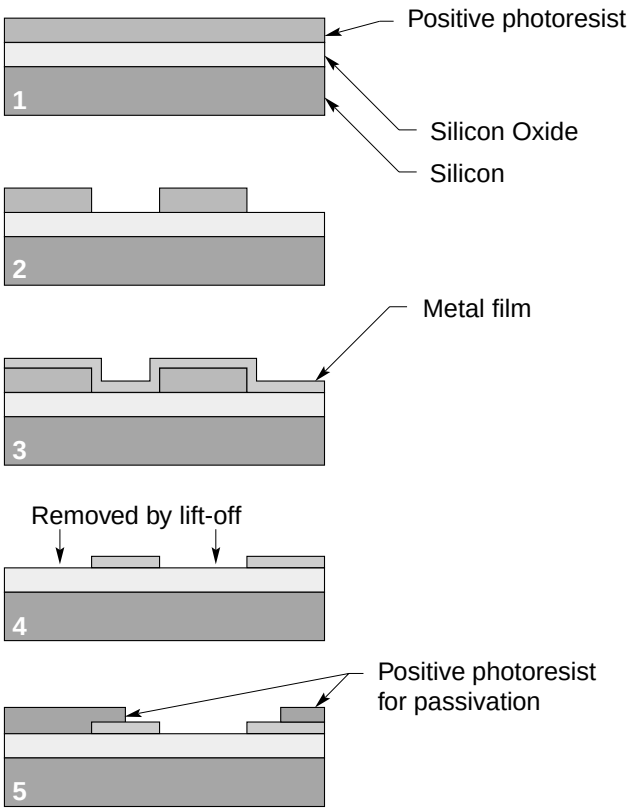

F2

Fabrication process of a carbon IDA electrode.

(1) Carbon film formation by pyrolysis on SiO_2 substrate.

(2) Lithographic patterning of photoresist.

(3) RIE patterning of carbon film.

(4) Removal of photoresist.

(5) Windowing by photoresist.

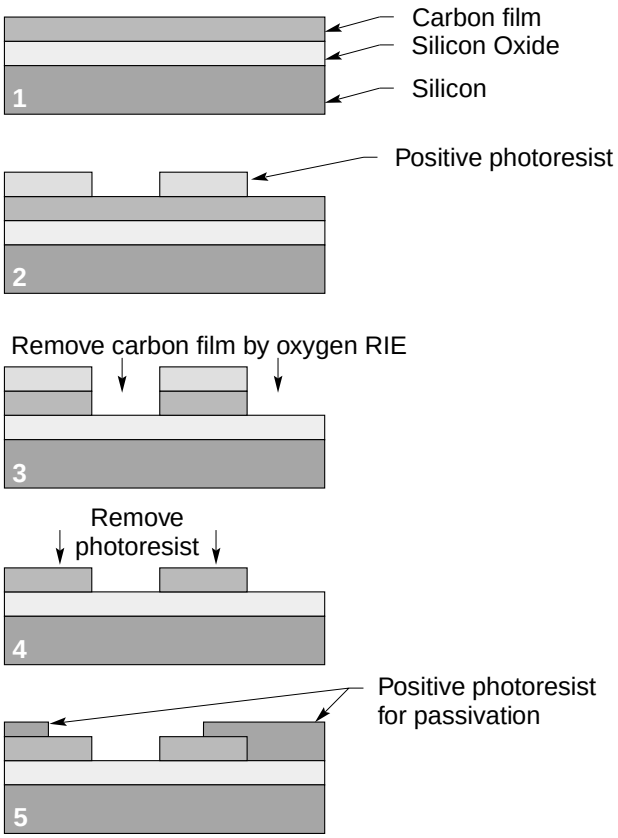

Fabrication of the IDA Electrode

Fabrication of the metal IDA electrode

The metal IDA microelectrode was fabricated on a silicon oxide covered silicon wafer using photolithography. The lift-off method was used to make the interdigitated metal electrode. The fabrication process was as follows (***F1***):

1. A positive photoresist was coated on an oxidized silicon wafer.
2. The resist film was exposed to UV light through a photomask using a contact mask aligner, and was developed in a resist developer and rinsed in deionized water.
3. Platinum or gold was sputter-deposited on the wafer to a thickness of about 100 nm, followed by the deposition of a thin titanium or chromium film (5 nm) with vacuum conditions maintained throughout.
4. The wafer was immersed in methylethylketone and the metalized resist pattern was lifted off.
5. A photoresist film was spin-coated, exposed, and developed. This pattern was used as a passivation layer after hardening by baking.

The fabricated electrode gap and width were 2 to 10 μm and the electrode length was 2 mm; 50 to 750 pairs of these microband electrodes were made on each wafer.

Fabrication of the carbon IDA electrode

The carbon-based IDA electrode was fabricated by pyrolysis of carbon precursor film and reactive ion etching (RIE) techniques. The fabrication process (14) was as follows (***F2***):

1. 3,4,9,10-Perylenetetracarboxylic dianhydride was pyrolyzed at 1373 K in 0.1 Torr and cast on an SiO_2-covered Si wafer. This

gave a metallic surface of conducting carbon film on the wafer.

2. A positive photoresist was coated on the carbon-covered wafer. The resist film was exposed through a photomask and developed.
3. The exposed area of carbon film was removed by O_2 RIE.
4. The photoresist was removed by a suitable solvent.
5. A photoresist film was spin-coated, exposed, and developed. This pattern was used as a passivation layer after hardening by baking.

F3

Experimental setup of dual-mode electrochemical experiments. A bipotentiostat is used to control two working electrodes (WE1, WE2).

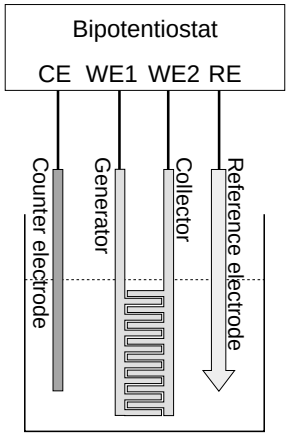

F4

Typical cyclic voltammogram of ferrocene. (a) IDA electrode operating in dual mode. I_a and I_c are steady-state current at the generator and the collector; I_0 is the limiting current of the generator without potentiostating the collector. (b) IDA electrode operating in single mode. The horizontal axis is generator potential.

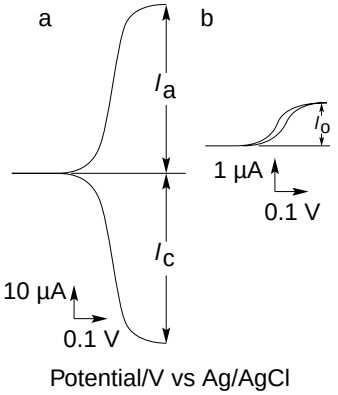

Electrochemical Characteristics of the IDA Electrode

Electrochemical method

Electrochemical measurements are carried out using a bipotentiostat to control the two working electrodes, as shown in ***F3***. In dual-mode cyclic voltammetry of the IDA electrode, one of the finger electrodes is held at a fixed potential (collector) and the other finger electrode is scanned (generator). The collector potential is set lower than the redox potential (usually < $E°$–100 mV) if the redox species is in the reduced form in solution.

Typical response of the IDA electrode

F4a shows a typical cyclic voltammogram of an IDA electrode operated in dual mode. As the generator electrode potential approached the redox potential, both collector and generator current increased by the same magnitude but with opposite sign ($I_a = -I_d$). When the generator potential surpassed the redox potential, both electrode currents became stable.

Dual/single mode comparison

When the collector is not potential-controlled (single mode), the current monitored at the generator electrode gives a sigmoidal or small peak-shaped curve, as shown in ***F4b***. The electrode areas of the collector and generator are the same in dual mode and single mode. The current is higher in dual mode than in single mode.

In dual mode, reduction and oxidation occur at very closely aligned electrodes. The product at one electrode becomes the source of the reaction at the adjacent electrode. This is called redox cycling, which is typical of twin microelectrodes (***F5***) (15–17).

The dependence of the dual-mode limiting current on the size of the electrode is shown in ***F6***. The redox cycle number is defined as the ratio of the limiting current (I_a or I_c) to I_0 (in ***F4***). The smaller the electrode, the higher the redox cycle number obtained. This effect is accelerated in micrometer size electrodes.

While redox cycling contributes to signal enhancement, the absence of a capacitive charging current at the collector electrode enhances the signal-to-noise ratio. In conventional cyclic voltammetric measurement, the magnitude of the charging current is linearly proportional to the potential sweep rate, and the faradaic signal current is proportional to the square root of the sweep rate. Therefore, a higher sweep rate gives a lower signal-to-noise ratio. When the IDA electrode is operated in dual mode, there is no charging current at the collector because the potential is fixed. Even when the potential scan rate is high and redox cycling becomes inefficient, the collector current is not affected by charging. Therefore, the IDA electrode is also suitable for high scanning speed voltammetry.

Mathematical analysis of dual-mode operation

The degree of current enhancement has been given mathematically (18). Solving a two-dimensional diffusional equation with suitable boundary conditions gives the limiting current I_{lim} of the IDA

F5

Current enhancement mechanism of redox cycling on an IDA electrode. R: reduced molecule. O: oxidized molecule.

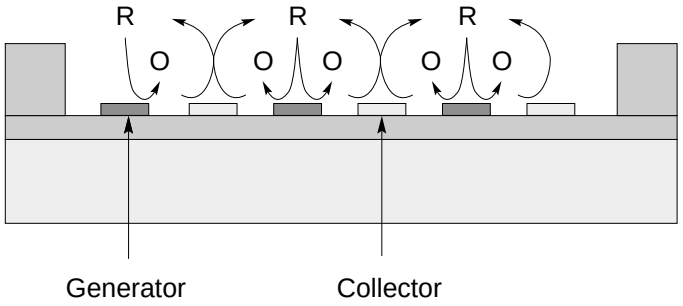

electrode in steady state. The analytical solution is

$$I_{lim} = 2mbnFC^*HD\frac{K(1-p)}{K(p)} \quad (1)$$

where $K(p)$ is a complete elliptic integral and p is a geometric parameter of IDA electrode alignment. Also, m is the number of microband electrodes, b is the length of the microband electrode of the IDA, n is the number of electrons involved in the redox reaction, F is the Faraday constant, C^* is the bulk concentration of the redox molecule, and D is the diffusion coefficient of the redox molecule (detailed definitions are given in ref. 18).

For practical use, equation 1 can be approximated as

$$I_{lim} = mbnFC^*D\left[0.637\ln\frac{2.55}{X} - 0.19X^2\right] \quad (2)$$

$$X = \frac{g}{w+g} \quad (3)$$

where g is the gap width and w is the band electrode width.

Equation 2 has been verified experimentally. In ***F7***, experimental data and the expected line from equation 2 are plotted.

The transient response (potential step chronoamperometry) of the IDA electrode has been calculated numerically. The IDA electrode reaches a steady state within 0.05 to $14 \times (w + g)^2/D$ seconds (19).

F6

Dependence of the redox cycle number on electrode size w/4+g where w is electrode width and g is electrode gap length.

● *aq-ferrocene*
○ *ferrocene*
▲ *ferrocyanide*
△ *ruthenium hexaammine*

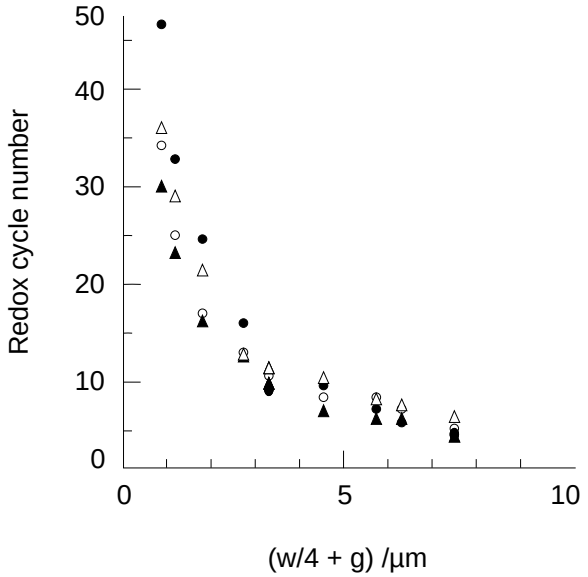

F7

Dependence of electrode dimension on limiting current.

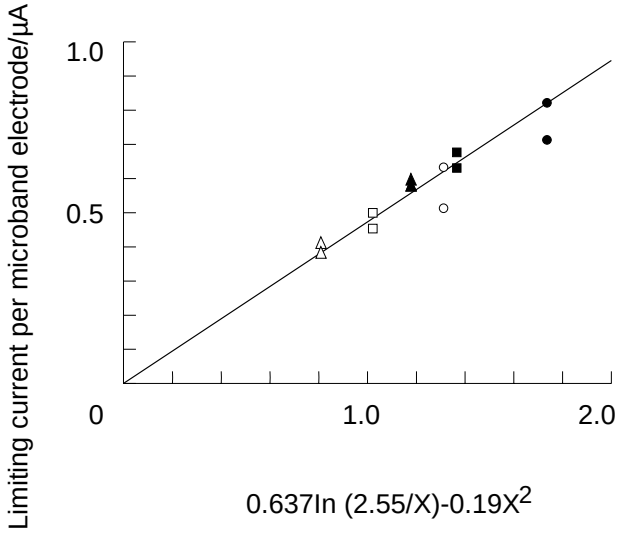

Dimensions of IDA electrodes:

Symbol	*w* (μm)	*g* (μm)	*b* (μm)	*m*
○	10.0	5.0	2.0	25
□	5.0	5.0	2.0	50
△	3.0	5.0	2.0	50
●	10.0	2.0	2.0	25

Self-induced redox cycling

Redox cycling can be induced by arranging electrode configuration and environment. When one side of the IDA electrode is relatively large or connected to a macroelectrode, current is enhanced without the need to control both electrodes. This is called self-induced redox cycling. ***F8*** shows the experimental scheme of this effect. The current at the controlled electrode is almost the same as expected by equation 2 when (ferrocenylmethyl)trimethylammonium (aq-ferrocene) is used. This effect is explained as follows: The oxidized form is produced at the potentiostated electrode (a) and becomes dominant locally; at the macroelectrode (c) connected to the other side of the IDA electrode (b), the concentration of the reduced form is dominant; because electrodes (b) and (c) are connected by an external circuit, the potential difference can be canceled by electron flow from (c) to (b); when surface concentration difference and potential differ-

F8

Schematic diagram for self-induced redox cycling. RE, reference electrode; CE, counter electrode; WE, working electrode. One of the fingers of the IDA electrode (b) is connected to a macroelectrode (c).

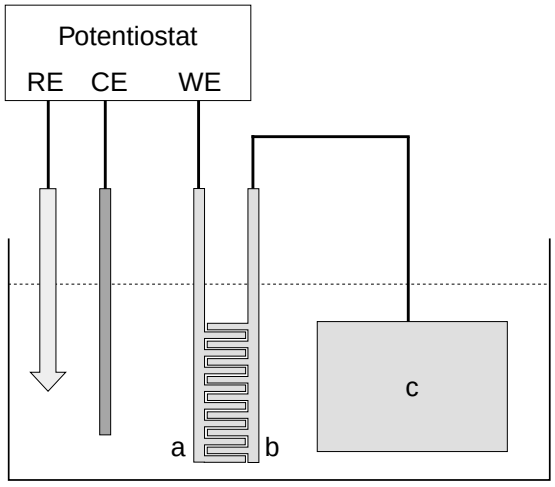

F9

Mechanism of substitutional stripping voltammetry (cathodic mode).

(1) Preelectrolysis of dissolved reversible species (analyte) at the twin electrode in cell compartment A induces preconcentration in cell compartment B. The two cells are connected by a salt bridge.

(2) Stripping stage on the macroelectrode.

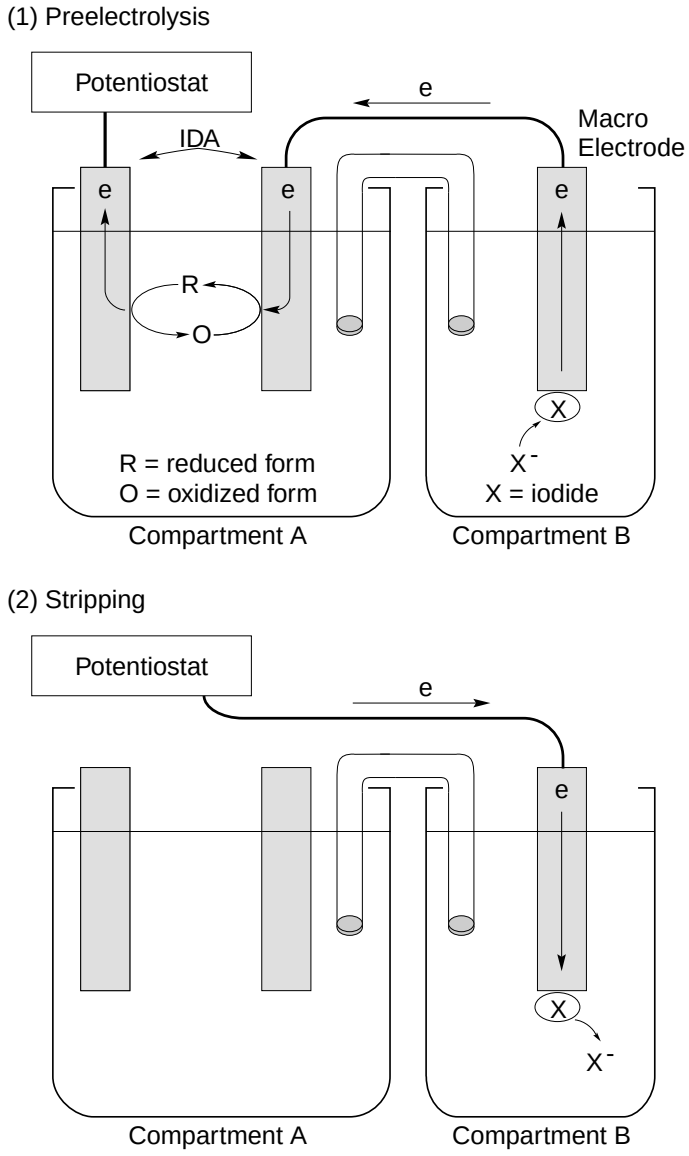

ence between (b) and (c) become zero, the total electron flow at (c) by oxidation is equal to that at (b) by reduction (20).

The self-induced redox cycling method requires one potentiostat, as in usual voltammetry, while dual-mode operation of an IDA requires a bipotentiostat. Hence, the former has the advantage of high-sensitivity analysis with simple equipment. This was demonstrated by a determination of dihydroxybenzylamine (an analog of a redox-active neurotransmitter). In this case, the lower limit of detection was as low as 100 nM. This is ten times lower than for a conventional single-mode measurement (21).

Substitutional Stripping Voltammetry (SSV) for high-sensitivity molecular recognition

A new type of stripping voltammetry has been developed that utilizes the self-induced redox cycling effect (20) for detecting trace amounts of electrochemically reversible redox species.

Substitutional Stripping Voltammetry (SSV) is achieved by combining an IDA electrode in an analyte solution in one cell compartment, A (***F9***), and a macroelectrode in another cell compartment, B, containing a redox species which deposits reversibly on the electrode.

The preelectrolysis of the reversible species at one finger set of the IDA electrode induces a reverse reaction at the other set. The charge produced by this reverse reaction is transmitted to the macroelectrode in the other cell (compartment B) through the outer circuit, and the electroactive species is deposited on the macroelectrode (***F9(1)***). When the potential of the macroelectrode is swept, the deposited material generates a highly amplified stripping current (***F9(2)***). The peak current is proportional to the redox species concentration in compartment A. The concentration of the redox species in an oxidized state can be measured using heavy metal ions (anodic mode); in a re-

F10

Typical calibration curve for dopamine on an IDA electrode (3 µm width, 2 µm gap).

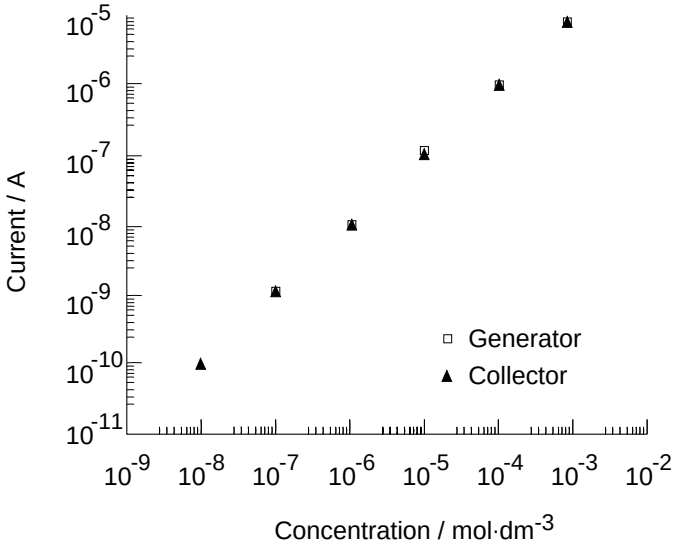

duced state, species can be measured using halides (cathodic mode) (22,23).

The magnitude of the signal can be controlled by changing the preelectrolysis time and the concentration of the depositing material. The value of the redox potential can be obtained by changing the preelectrolysis potential.

The theoretical current of a single electrode whose electrode area is the same as the total IDA area is 0.1 nA for 10 nM redox species, when calculated at a sweep rate of 20 mV/sec in conventional cyclic voltammetry. On the other hand, the peak current from SSV for the same sample is 250 nA, which is 2500 times larger than obtained by cyclic voltammetry with a single electrode of the same size. The detection limit of 10 pM (2 ppt) for rutheniumhexaammine by SSV has been reported (22).

Applications

As described in previous sections, the narrow-gap IDA offers high sensitivity and short response time. The IDA electrode also has a small sample volume requirement for practical measurements. These characteristics make IDA electrodes suitable for the detection of biological substances and for detection in liquid chromatography (LC) or flow injection analysis (FIA).

Detection of biological substances

Application of the IDA electrode for quantitative analysis of dopamine, which is one of the most important neurotransmitters, has been reported (24). In this case, the influence of interferents such as ascorbic acid can be removed by oxidation at one electrode to an electrochemically inactive species. A typical calibration curve of dual-mode IDA measurement for dopamine is shown in ***F10***. The oxidized form of dopamine is unstable, but at the narrow gap IDA electrode, dopamine can be quantitatively determined because the oxidized form is rapidly reduced before it becomes the redox-inactive form. The linear range extends for five digits. This versatile performance supports the applicability of IDA for quantitative analysis of a small amount of a reversible redox species.

For practical usage, a large number of finger IDA electrodes have been fabricated and integrated in the detection cell of an LCEC system. The detection limit of this system is reported as 100 pM for dopamine (25).

Sub-femtomole detection of dopamine with an IDA carbon microelectrode

Electrochemical detection is important in LC, especially for neurochemical substances. By incorporating the carbon IDA electrode into a microbore LC system, small volume and low-concentration analysis of biological samples is feasible. The combination of IDA electrode and microbore column is ideal in this scheme because the sample volume can be reduced and the flow rate, which is slower than in an ordinary size column, sustains high collection efficiency. A carbon electrode has a wider potential window and larger overpotential for water than noble metal electrodes, and is expected to improve sensitivity for redox-active biological molecules because in most cases their electrochemical reaction is slow on a metal electrode.

F11 shows anodic chromatograms of dopamine obtained using the IDA carbon microelectrode. The detection limit of 0.5 fmol for 5 µL of dopamine (100 pM) is reported with an IDA electrode consisting of 300 pairs, 5-µm finger widths and gaps, and 2-mm finger length (26). A lower detection limit can be expected if a smaller IDA carbon microelectrode and a smaller volume sample are used.

Conclusion

The operating mechanism and theoretical explanation of an IDA electrode fabricated by a lithography technique has been described. The high-sensitivity analysis attained by an IDA electrode has been demonstrated.

It has been found that the IDA electrode not only has high sensitivity but also has high selectivity by proper design of its shape. This is a kind of chemical filter that picks up objective reactant from side reactions. It is therefore expected that the IDA electrode will become part of an intelligent electrochemical system. Furthermore, microelectrodes are suitable for electrochemi-

F11

Anodic chromatograms of low-concentration dopamine on a carbon IDA electrode incorporated in an LCEC system.

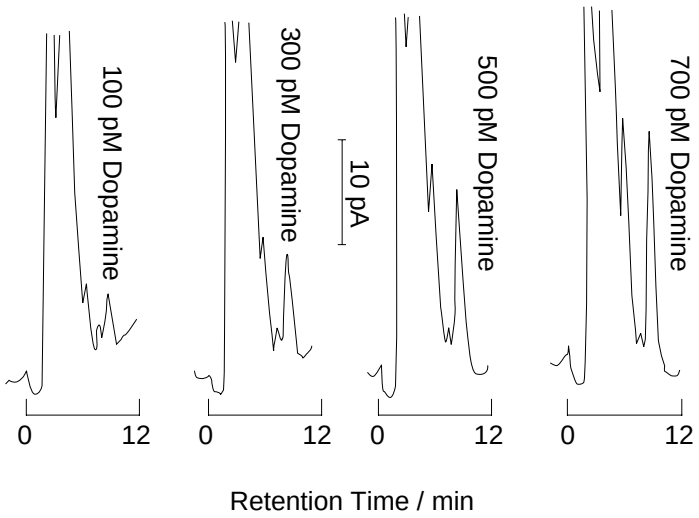

cal experiments in nonpolar solvents, low-conductivity solvents, and ion-conductive polymers, in which macroelectrodes cannot be used because of their significant potential drop. Moreover, enzyme modification of microelectrodes or integration of immunoreaction with electrochemical reactions will widen the variation of measurement. Microelectrodes are expected to spread into many analytical fields in the near future.

Acknowledgments

The authors gratefully acknowledge O. Niwa, T. Horiuchi, and H. Tabei for their suggestions in preparing this manuscript.

References

1. *M. Fleischmann, S. Ponds, D. Rolinson, and P.P. Schmidt, Ultramicroelectrodes, Datatech Science, Morganton, NC, 1987.*
2. *K. Aoki, Denki Kagaku 56 (1988) 608.*
3. *J. Janata and A. Bezegh, Anal. Chem. 60 (1988) 62R.*
4. *J.O. Howell and R.M. Wightman, J. Phys. Chem. 88 (1984) 3915.*
5. *L. Geng, A.G. Ewing, J.C. Jernigan, and R.W. Murray, Anal. Chem. 54 (1986) 852.*
6. *E.T.T. Jones, O.M. Chyan, and M.S. Wrighton, J. Am. Chem. Soc. 109 (1987) 5526.*
7. *K. Aoki, Electroanalysis 5 (1993) 627–639.*
8. *D.G. Sanderson and J.L. Anderson, Anal. Chem. 57 (1985) 2388.*
9. *C.E. Chidsey, B.J. Feldman, C. Lundgren, and R.W. Murray, Anal. Chem. 58 (1986) 601.*
10. *L.E. Fosdick, J.L. Anderson, T.A. Baginski, and R.C. Jaeger, Anal. Chem. 58 (1986) 2750.*
11. *B.J. Feldman and R.W. Murray, Anal. Chem. 58 (1986) 2844.*
12. *F. Mansfield, J. Electrochem. Soc. 135 (1988) 1354.*
13. *See references 14–18, 20–26.*
14. *H. Tabei, M. Morita, O. Niwa, and T. Horiuchi, J. Electroanal. Chem. 334 (1992) 25.*
15. *O. Niwa, M. Morita, and H. Tabei, J. Electroanal. Chem. 267 (1989) 291.*
16. *T. Horiuchi, O. Niwa, M. Morita, and H. Tabei, J. Electroanal. Chem. 295 (1990) 25.*
17. *O. Niwa, M. Morita, and H. Tabei, Anal. Chem. 62 (1990) 447.*
18. *K. Aoki, M. Morita, O. Niwa, and H. Tabei, J. Electroanal. Chem. 256 (1988) 269.*
19. *K. Aoki and M. Tanaka, J. Electroanal. Chem. 266 (1989) 11–20.*
20. *T. Horiuchi, O. Niwa, M. Morita, and H. Tabei, J. Electrochem. Soc. 138 (1991) 3549.*
21. *H. Tabei, T. Horiuchi, O. Niwa, and M. Morita, J. Electroanal. Chem. 326 (1992) 339.*
22. *T. Horiuchi, O. Niwa, M. Morita, and H. Tabei, Anal. Chem. 64 (1992) 3206.*
23. *T. Horiuchi, O. Niwa, M. Morita, and H. Tabei, Denki Kagaku 60 (1992) 1130.*
24. *O. Niwa, M. Morita, and H. Tabei, Electroanalysis 3 (1991) 163.*
25. *M. Takahashi, M. Morita, O. Niwa, and H. Tabei, J. Electroanal. Chem. 335 (1992) 253.*
26. *H. Tabei, M. Takahashi, S. Hoshino, O. Niwa, and T. Horiuchi, Anal. Chem. 66 (1994) 3500.*